JAAS

RSC Publishing

PAPER

View Article Online
View Journal | View Issue

Synchrotron-based chemical imaging reveals plumage patterns in a 150 million year old early bird

Cite this: *J. Anal. At. Spectrom.*, 2013, **28**, 1024

Phillip. L. Manning,*[a] Nicholas P. Edwards,[a] Roy A. Wogelius,*[a] Uwe Bergmann,[b] Holly E. Barden,[a] Peter L. Larson,[c] Daniela Schwarz-Wings,[d] Victoria M. Egerton,[a] Dimosthenis Sokaras,[b] Roberto A. Mori[b] and William I. Sellers[e]

Charles Darwin acknowledged the importance of colour in the natural selection of bird plumage. Colour can indicate age, sex, and diet, as well as play roles in camouflage, mating and establishing territories. Feather and integument colour depend on both chemical and structural characteristics and so melanosome structure and trace metal biomarkers can be used to infer colour and pigment patterns in a range of extant and fossil organisms. In this study, three key specimens of *Archaeopteryx* were subjected to non-destructive chemical analysis in order to investigate the potential preservation of original pigmentation in early fossil feathers. Synchrotron Rapid Scanning X-ray Fluorescence (SRS-XRF) maps are combined with sulphur X-ray Absorption Near Edge Structure (XANES) spectroscopy to provide the first map of organic sulphur distribution within whole fossils, and demonstrate that organically derived endogenous compounds are present. The distribution of trace-metals and organic sulphur in *Archaeopteryx* strongly suggests that remnants of endogenous eumelanin pigment have been preserved in the feathers of this iconic fossil. These distributions are used here to predict the complete feather pigment pattern and show that the distal tips and outer vanes of feathers were more heavily pigmented than inner vanes, contrary to recent studies. This pigment adaptation might have impacted upon the structural and mechanical properties of early feathers, steering plumage evolution in *Archaeopteryx* and other feathered theropod dinosaurs.

Received 6th March 2013
Accepted 31st May 2013

DOI: 10.1039/c3ja50077b

www.rsc.org/jaas

Introduction

Darwin[1] drew much attention to the artificial selection of plumage colour in domestic pigeons (*Columba livia*) in the absence of a mechanism (genetic) to explain this variation. The selective breeding of pigeons into many diverse forms and colours aided Darwin's understanding of natural selection through descent with modification. Our understanding of colour, form and function of feathers has been further expanded since the genetic mechanisms behind their natural selection were identified.[2] The colour of bird plumage is a function of selection processes and can vary depending on age, sex and mode of living; and also play important roles in camouflage, mating and the establishment of territories.[3]

Melanin pigments are the most widely used pigments in birds[4] and are found in vertebrates within almost all types of integument structures including hair, skin and eyes.[5] Melanin pigments consist of several covalently linked indoles and are considered to be unusually large polymers compared to most natural pigments.[6] The sheer size and complexity of these molecules determines their precise structure and their physical properties and controls their bonding to other components (*e.g.* proteins, metal ions). These heterogamous polyphenol-like biopolymers vary in colour from yellow to black.[7] There are two main melanin pigments in animal tissues, eumelanins and pheomelanins. The former are more prevalent (>75%) and furnish dark, black or brown hues in both invertebrates and vertebrates.[8] There is variation in size between the two main melanin molecules, with eumelanin forming larger, rod-like granules that are insoluble in almost all solvents. Pheomelanins, in contrast, form the reddish-brown pigments. They are smaller, globular granules compared to eumelanin and are soluble in alkaline solutions.[9] Pheomelanins also have different light absorbance and structural characteristics to eumelanins. However, Ito (2003)[10] suggested that eumelanin is deposited on preformed pheomelanin and that the ratio of the two is determined by tyrosinase activity and cysteine concentration.

All birds deposit some melanin in their feathers, with the rare exception of albino forms. Melanization of avian tissues can vary due to season, intraspecifically and sexually relative to

[a]*University of Manchester, School of Earth, Atmospheric, and Environmental Sciences, Manchester, M13 9PL, UK. E-mail: phil.manning@manchester.ac.uk*

[b]*SLAC National Accelerator Laboratory, Linac Coherent Light Source, Menlo Park, CA, 94025, USA*

[c]*Black Hills Institute of Geological Research, Inc., Hill City, SD, 57745, USA*

[d]*Museum für Naturkunde, Leibniz Institute for Research on Evolution and Biodiversity, Berlin, Germany*

[e]*University of Manchester, Faculty of Life Sciences, Manchester, M13 9PT, UK*

other forms of colouration (physical and carotenoid). Typically the head, breast, throat and neck of many birds exhibit distinct melanization. Furthermore, the relative amount and spatial distribution of melanin in feathers can also vary, with some species concentrating melanin in upper, but not lower surfaces of feathers.

Studies on the elucidation of colour in fossil feathers[11–13] have suggested that the presence of melanosomes within fossil feathers may be used to tentatively to reconstruct feather colours by tracking variations in melanosome shape. Rod shapes were interpreted as eumelanosomes (dark black/brown) and spheroidal shapes as pheomelanosomes (reddish-brown). This structural approach has some shortcomings, primarily that there is known diversity in melanin granule morphology among different species[3,14] and melanosome preservation may not be uniform. Therefore, serious questions may be raised about colour interpretation based solely on fossilised melanosome morphology and distribution.[11,12,15] Additionally, these studies did not account for other known contributors to colour in feathers, such as the possible presence of other pigments (*e.g.* carotenoids) or other physical structures.[4]

Wogelius *et al.*[16] used a non-destructive chemical approach to investigate fossil pigments. Using SRS-XRF imaging combined with X-ray absorption spectroscopy, they were able to chemically map the presence of eumelanin trace-metal biomarkers (organometallic Cu chelates) in samples from birds (feathers), cephalopods (ink sac) and fish (eyes). It was also observed that there was a strong correlation with melanosome presence (when preserved) and Cu distribution on both fossil and extant feathers. This work clearly demonstrated the importance of sample chemistry when mapping pigments in both extant and fossil samples. Copper (Cu) XANES spectroscopy was used to precisely diagnose the presence of eumelanin derived Cu in the feathers of the earliest bird, *Archaeopteryx*, but pigment distribution and density across the whole sample was not determined in this earlier study.[16]

Archaeopteryx is a pivotal species to our understanding of bird evolution, but fossils of this animal are extremely rare, known only from eleven specimens that have been collected from the Late Jurassic (150 million year old) Solnhofen Limestone of southern Germany.[17] The first *Archaeopteryx* fossil found consists of a single feather, comprising part and counterpart, held in Munich (BSP-1869-VIII-1) and Berlin (MB.Av.100), respectively.[18–20] MB.Av.100 is preserved as a dark carbonaceous film suggestive of organic material[17] (Fig. 1A) and specimen BSP-1869-VIII-1 (Fig. 2) shows a fainter distribution of organic material, but retains the darker distal tip.[17] The same distribution of organic residue on both parts shows that the zonation seen in MB.Av.100 is genuine and not an artefact of an uneven split of the fossil between adjacent bedding surfaces. The other *Archaeopteryx* specimens show little or no visible evidence of soft tissue residue despite the visible evidence of feathers ('impressions').[4] While much is known of the morphology of this early bird,[17] little has been published of the chemistry from these fossils until recently.[13,21]

The exceptional preservation of MB.Av.100 and BSP-1869-VIII-1 (Fig. 2) suggests the potential presence of endogenous melanin pigments and/or their breakdown products.[13,22] Recent work on melanosome morphology suggests that the pigment in *Archaeopteryx* feathers was most probably black.[13] However, the current studies of melanosome morphology rely on point sampling and predict the presence and colour of pigment at discrete locations. These approaches are therefore unable to quantify the intensity/distribution of feather pigment over a complete fossil. The use of structural information for diagnosing pigmentation[11–13] relies on the assumption that there is a correlation between the quantity of preserved melanosomes and pigment density, and does not consider chemical changes such as structural breakdown. Recent studies have shown that there are indeed variations in chemistry, and it is this chemical variation that more robustly resolves the presence, concentration, and pigment pattern.[16] Given the irreplaceable scientific

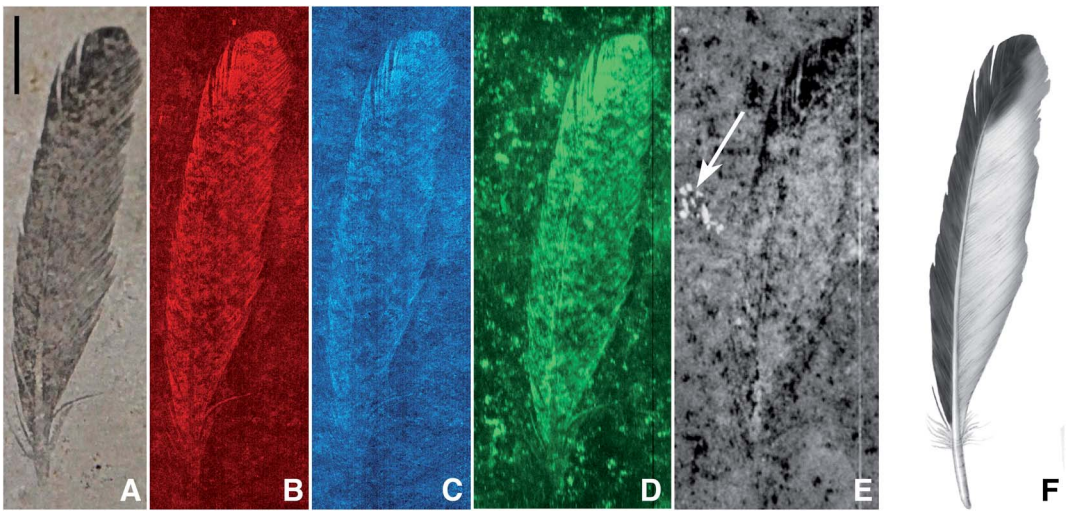

Fig. 1 *Archaeopteryx lithographica* single feather (MB.Av.100), visible light (A), SRS-XRF false colour images of copper (B), nickel (C), organic sulphur (all species) (D), sulphate only map (E) and artist's restoration (F). The white arrow on (E) indicates the presence of sulphate in a fossil bone fragment just below the sediment surface (scale bar = 10 mm). Brighter equates to increased concentration.

Fig. 2 Mb.Av.100 (Berlin feather counterpart) and BSP-1869-VIII-1 (Munich feather part) specimen (counterpart and part respectively), with the Munich specimen image mirrored. Specimen MB.Av.100 is preserved as a dark carbonaceous film suggestive of organic material and the counter specimen BSP-1869-VIII-1 shows a fainter distribution of organic material, but retains the darker distal tip. This confirms that any zonation seen in the counterpart (MB.Av.100) is genuine and not an artefact of an uneven split of the fossil between adjacent bedding surfaces.

and cultural value of all *Archaeopteryx* specimens, no destructive chemical analysis is possible to verify these earlier findings. However, SRS-XRF has been shown to non-destructively resolve fossil chemical zonation patterns,[21,23] including metal biomarkers for eumelanin pigmentation.[16] Here we use SRS-XRF and XANES spectroscopy to investigate the chemical composition of three *Archaeopteryx* specimens (MB.Av.100, HMN1880, and WOCCSG100) to determine whether endogenous pigments are preserved and if so, resolve their density and distribution.

Methods

The specimens were analysed using X-ray fluorescence on beamline 6-2 at the Stanford Synchrotron Radiation Light source (SSRL, CA, USA). X-ray fluorescence mapping was performed by mounting the specimens vertically on an *x*–*y* scanning experimental stage and rastered in front of the fixed incident X-ray beam.[21,24] Two separate scans of each specimen were made, one using an incident beam energy of 13.5 keV in order to induce k-line X-ray emission from heavier atomic weight elements (such as Cu and Ni), the other using an incident beam energy of 3.15 keV to investigate lighter atomic weight elements (such as S and P). For high *Z* mapping the stage was aligned at a fixed incident angle of 45° with a single element drift detector (vortex) set at 90° scattering angle relative to the incident beam. For low *Z* mapping, the scattering angle was ~160° and specimens were housed in a helium atmosphere to minimize signal loss from air absorption of both the incident beam and fluoresced X-rays. Fluoresced X-ray energy regions of interest were set electronically to capture characteristic elemental emission line intensities. For all maps (except organic sulphur) beam spot size on the sample was produced using either 100 μm or 20 μm diameter circular pinhole apertures.

Point analyses were taken on each sample to allow us to apply a concentration scale to the maps and also provide well-constrained measurements of elemental abundances at various points within the specimens and matrices. As with the images, point analyses were made at incident energies of both 3.15 and 13.5 keV. Point analyses were completed by driving the rapid scanning stage to a location of interest defined by previously acquired maps, counting for 100 seconds (as compared to the ~3.3 ms per pixel used in rapid scanning), and acquiring a full energy dispersive spectrum at each point. We note that limits of detection are several atomic weight percent for low atomic weight elements, decreasing to approximately 1 ppm for heavier elements. Elemental concentrations were calculated from the raw spectral data using the ESRF developed PyMCA freeware by directly measured fundamental parameters including but not limited to: flux, detector distance, analysis time, *etc.* Point analyses were obtained at both incident beam energies (3.15 keV and 13.5 keV) and a Durango apatite mineral standard and known Ca concentrations of the Solnhofen Limestone were used as reference/calibration materials to estimate errors (for full explanation of the point analyses protocol see Bergmann *et al.*[21]).

XANES spectra were recorded in fluorescence mode. XANES spectroscopy is sensitive to the electronic structure of the probed central absorber atom, especially to oxidation state and coordination number. Calibration of the incident beam energy for XANES and sulphur oxidation state mapping was accomplished by analyzing a K_2SO_4 standard. XANES peaks were identified by comparison to those published in the literature.[25] For mapping of discrete sulphur oxidation states, the incident beam energy was set by monochromator rotation to the resonance energies of specific sulphur species identified by XANES. The map of organic sulphur was obtained by setting the incident beam energy to below the inorganic sulphate edge (2479.9 eV) thus eliminating any contribution from sulphate. Image subtraction was employed to produce the inorganic sulphate only map (map at 2479.9 eV was subtracted from the map taken at the sulphate absorption edge 2481.5 eV). For these scans the pinhole was removed in order to maximize flux, resulting in ~500 μm spot size. Velocirastor software and MATLAB were used to generate elemental maps from the collected data (raster files) and also aligned each scan. ImageJ built in image calculator was used to subtract the images in

order to produce the sulphate only map. The Image CorrelationJ plugin for ImageJ was used to provide correlation coefficients for inorganic/organic sulphur and copper/organic sulphur.

Results

SRS-XRF maps of copper, nickel, and organic sulphur faithfully replicate the feather structure of MB.Av.100 (Fig. 1). Trace-metal distribution in the feathers of HMN1880 (counterpart) was comparable to that seen in MB.Av.100 with elevated levels of Cu in the outer vane (leading edge) and tip of the feather (Fig. 3). The SRS-XRF maps of WDCCSG100 did not detect copper or nickel in the feathers,[21] but were able to spatially resolve feather structure in iron, phosphorus and sulphur. Interestingly, elevated levels of Ca and P occur in a small area, only a few millimetres in size, detected just a few tens of microns below the matrix surface of specimen MB.Av.100 (Fig. 1E). The elevated levels of P and Ca are comparable to prior studies of *Archaeopteryx* bone chemistry (Fig. 4).[21]

XANES K-edge analysis of sulphur in MB.Av.100 allows sulphur oxidation states to be determined (Fig. 1D and E). The distribution of sulphur is subtly different in the feather when compared to the matrix, with elevated organic thiol and sulphoxide (comparable to cysteine and methionine sulfoxide) concentration in the feather as might be expected for keratin derived material (Fig. 5). Inorganic sulphate is weakly correlated with organic sulphur species (Fig. 1E). Furthermore, Cu, Ni, and organic S are not uniformly distributed within the feather, but all correlate with each other, showing enrichment within the outer vane and distal tip (Fig. 1B and C). The maps for the distribution of organic sulphur (2479.9 eV) and inorganic sulphate at (2481.5 eV) in MB.Av.100 were compared in ImageJ (using the CorrelationJ plugin) and a correlation coefficient of R^2 0.17 was produced. A correlation coefficient of R^2 0.48 was also calculated for Cu and organic sulphur from a masked area at the tip of MB.Av.100. XRF point analyses quantify the concentrations of Cu, Ni, P, and S in MB.Av.100 (Table 1).

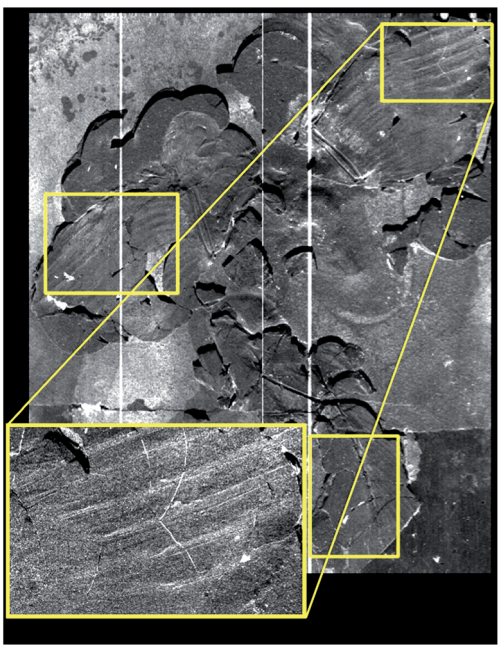

Fig. 3 SRS-XRF image of Berlin *Archaeopteryx* counterpart (HMN1880) showing the distribution of copper. Boxed regions of interest (yellow) mark areas where the bilateral symmetry of copper distribution in the outer vane (leading edge) is elevated when compared to the inner vane (posterior edge), but also maintained in the feather tips.

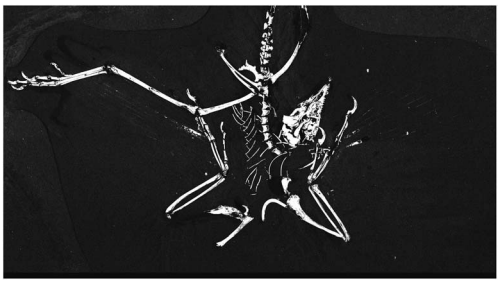

Fig. 4 SRS-XRF phosphorus map of the Thermopolis *Archaeopteryx* (WDCCSG100).

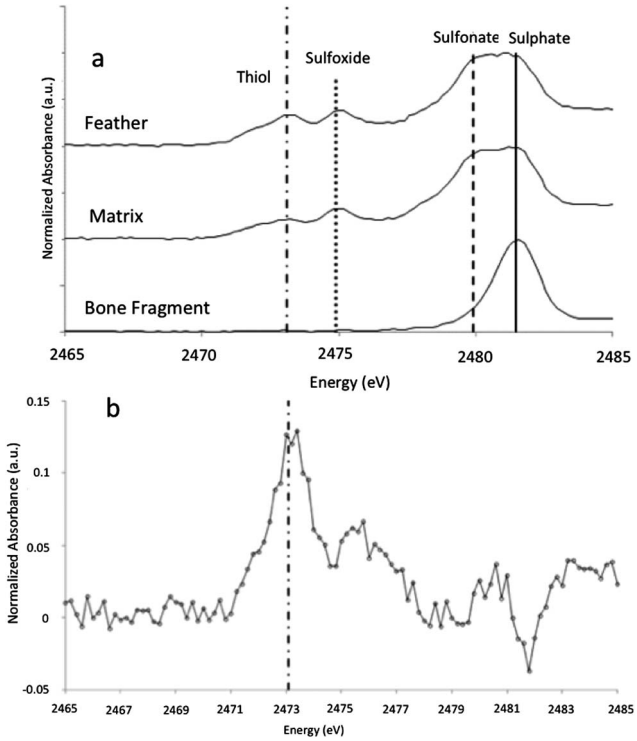

Fig. 5 (a) XANES analyses of sulphur present within the feather compared to the sedimentary matrix and a small bone fragment present within the sample. The feather spectrum is obviously different from the bone fragment that shows only inorganic sulphate. The inorganic sulphate and other organic sulphur species (with peak energies equivalent to theoretical values for methionine sulphoxide and sulphonate and cysteine) in the matrix are either foreign material or keratin-derived oxidation products from un-pigmented parts of the feather, diffused away from the feather itself. Higher sulphur levels in the feather relative to the matrix (Table 1) strongly imply mass transfer of sulphur was from the feather outwards. (b) Difference spectrum of sulphur species for the feather minus the matrix, showing that the feather has a distinct sulphur inventory relative to the matrix with much higher thiol concentrations and lower sulphate, consistent with the presence of beta-keratin derived residue.

Table 1 XRF point analyses on *Archaeopteryx* specimen MB.Av.100. Errors (2σ) are approximately ±0.3 wt% for S, ±150 ppm for P, and ±10 ppm for Cu and Ni

Point location	S	P	Cu	Ni
Feather tip	7753 ppm	1732 ppm	37 ppm	34 ppm
Feather base	5254 ppm	2706 ppm	21 ppm	8 ppm
Matrix	1912 ppm	1385 ppm	3 ppm	4 ppm

The XRF point analyses presented in Table 1 provide important quantification of the chemical zoning observed in the SRS-XRF imaging maps (Fig. 1).

Discussion

A previous study has shown that the K-edge XANES spectrum of Cu within MB.Av.100 displays features comparable to it being organically bound, particularly resembling Cu bonded to natural eumelanin.[16] These results were inconsistent with the presence of geochemical precipitates such as Cu oxides or sulphides as a host for Cu in this case, and indicated that Cu is most likely present in MB.Av.100 as an organic copper chelate. SRS-XRF of WDCCSG100 has shown that the chemical remains of flight feather rachises are identifiable by the distribution of P and S.[21] The P and S levels (310 ppm for P and 65 ppm for S) present in the rachises of WDCCSG100 did not require transfer from the enclosing matrix, as these concentrations were well within the documented range observed in extant feathers.[21] The P and S levels determined for MB.Av.100 are greater than those seen in WDCCSG100 but this is most likely due to the higher amount of organic residue preserved compared to WDCCSG100.

Sulphur concentrations derived from keratinous integument, such as feathers, should be relatively constant yet here we observe that organic sulphur (Fig. 1D) correlates with trace metal zonation (Fig. 1B and C). A correlation analysis of Cu with organic S for MB.Av.100 shows that there is a positive correlation ($R^2 = 0.48$) (Fig. 1B and D). We argue that the uneven preservation of organic sulphur correlating with Cu, is a result of the biocidal properties of chelated metals as seen in extant feathers,[26] reducing local breakdown of organic sulphur from the original feather keratin. The weak, but still positive correlation coefficient for the distribution of organic sulphur relative to inorganic sulphate (Fig. 1D and E) is not surprising for such ancient samples.

Davis and Briggs (1998)[27] indicate that in a relatively short period of time (~10 days reaction time) feathers may undergo a 90% loss of mass. This process might concentrate any organically bound trace metals originally within the keratin into the more stable melanin. Despite documented resistance of soft tissues to degradation[16,23,28] we must consider that the work by Davis and Briggs (1998),[27] along with other experimental studies, has concluded that degradation will become severe rapidly under anaerobic conditions.[29] This would force one to conclude that rapid contemporaneous mineralization could be the only pathway leading to fine scale textural survival.[30] Those experimental studies, however, were completed under conditions of constant saturation with constant high microbial activity. Metal loadings were not reported. In contrast to those studies, recent work[31,32] examining soft tissue breakdown over extended periods (2 to 4 years) suggests that dehydration early in the taphonomic history of a specimen may shut down anaerobic breakdown processes. This recent work also suggests that keratin has a higher preservation potential than collagen. Considering these factors, we conclude that trace metal-bearing melanised tissue may be extremely resistant to anaerobic decay and, under the right conditions, may allow soft tissue to survive even under re-saturated conditions for extended periods.

Copper (or Fe, Ni, Zn, Ca) added by geochemical processes could also react with organic residue and become melanin chelated, although the levels we report here do not require additions from geochemical sources. Melanin is capable of incorporating as much as 3–6% by weight copper.[33] Therefore, if early or late stage geochemical processes added copper, one would have to explain why uptake of copper stopped at concentrations 2 to 3 orders of magnitude lower than saturation. It is possible that Cu-chelation could decrease the thermodynamic activity of Cu in solution locally and this may drive Cu release from nearby minerals without large-scale transport. This would then make incorporation a diffusion limited process rather than an advective process which, in any case, would only contribute a small amount of Cu. However, this would leave a transition metal depleted zone surrounding the fossil and we do not observe such a feature here. We cannot, however, unequivocally rule out some geochemical addition. At the onset of anaerobic degradation melanin would be unsaturated with metal, and so as keratin and the rest of the soft tissue breaks down and releases metals (Cu, Ni, Zn and Ca especially) they may form additional melanin-chelates, concentrating any original organically bound metals into melanin. However, the Cu levels quantified in the fossils here can be explained by normal Cu levels in the original organism. Cu concentrations determined for MB.Av.100 are comparable to concentrations measured within melanosomes of modern organisms.[34] Adding the fact that the Cu bonding environment is consistent with organic chelation, we conclude that the observed trace-metal zoning in the feathers of *Archaeopteryx* is due to breakdown products from within the original melanin, originally present mostly as a melanin-chelate but also complexed with tyrosinase or keratin[16] (although there is a possible contribution from other organic chelates present in the soft tissue). Concentration of Cu and Ni at the feathers distal tip and outer vane indicates that those portions were more heavily pigmented than the inner vane (Fig. 1E) so based upon the trace-metal distribution we suggest similar patternation for HMN1880 (Fig. 3).

This explains the original presence and retention of trace-metals by melanin in the early stages of degradation, but does not explain how soft tissue and metal biomarker distribution survive anaerobic decay over geologic time. Two aspects of feather chemistry play a role in preservation. First we note that copper sulphate has been used as an algaecide for over 100 years. Cu levels of 10 ppb have been shown to reduce bacterial colony-forming units by as much as 2 orders of magnitude.[35] This would suggest that copper inhibits bacterial degradation

hence could also act to enhance fossil preservation, especially of soft tissue such as feathers. Secondly, the presence of melanin itself in feathers may play a key role in their preferential preservation relative to soft tissue with low melanin content. In a recent study[35] the black and white feathers of domestic chickens were exposed to feather-degrading bacteria (*Bacillus licheniformes*). The white feather broke-down significantly faster than the black melanised feathers. This result was corroborated by a study on house sparrows (*Melospiza melodia*).[36] Both studies suggest plumage colour might be an evolutionary response to the presence of feather-degrading bacteria, with high melanic content being more resistant to decay.

The penetration depth of the SRS-XRF incident X-ray beam below the surface of the matrix slab revealed the presence of a small bone fragment buried on the order of several microns below the surface (Fig. 1E marked with white arrow). This is the first record of any bone to be associated with the single feather (MB.Av.100). XRF point analysis of the bone fragment indicates it has a comparable elemental inventory to that of the *Archaeopteryx* WDCCSG100,[21] and XANES analysis (and image subtraction) shows that the sulphur inventory in the bone fragment was almost entirely sulphate, again identical to the results for sulphur within bone from WDCCSG100. The holotype status of MB.Av.100 was recently revoked, on the basis that it was not identifiable to a specific species and could belong to any taxon of fossil bird from Solnhofen.[37] The chemical affinity of this small bone fragment and feather trace-metal inventory could lend support to the feather retaining holotype status, given that it can now be associated by two independent elemental inventories comparable to a known skeleton of WDCCSG100 (ref. 21) and feathers of HMN1880. However, additional evidence from remaining *Archaeopteryx* specimens and other vertebrates from Solnhofen is required to verify this interpretation.

Curatorial artefacts are also clearly resolved *via* SRS-XRF scanning of Mb.Av.100, HMN1880 and in WDCCSG100 (ref. 21). In particular, Zn has been added to the periphery of the rock slab of the two specimens from Berlin (Mb.Av.100 and HMN1880), probably through the use of adhesives and possibly transferred from the brass collection drawer handles used in the museum stores during handling. This shows the importance of large-scale chemical characterisation and imaging when compared to more traditional SEM-based techniques. Such small-scale analysis would not be able to resolve the total distribution of Zn and could mistakenly be interpreted as having had an endogenous origin. However, with the synchrotron-based imaging applied in this study, we can confidently differentiate between contamination and endogenous element loadings (in this case, Zn) in our analysis.[16] SRS-XRF results indicate that the fossil inventory of Cu, Ni, or S in MB.AV.100 has not been directly affected by curatorial processes. Scans of the entire specimen surface show that the Cu and Ni patterns are not associated with any contaminates.

The SRS-XRF work presented here broadly agrees with UV-light studies,[22] and refines the interpretation based on discrete point analyses of melanosome shape.[13] Carney *et al.*[13] also claimed to have identified organic sulphur in MB.Av.100; however, the techniques employed in their study could not have distinguished between different forms of sulphur; therefore, they only observed total sulphur. Resolving organic and inorganic sulphur can easily be achieved using synchrotron-based imaging techniques, so this study is the first to quantify and spatially resolve the presence of exclusively organic sulphur within MB.Av.100 by combining XANES analysis and SRS-XRF.

Conclusion

Our results show that in order to resolve feather colour in fossils, a combination of both structural and chemical analyses is necessary. Structural electron microscope based approaches to diagnosing colour typically rely upon data collected from less than 1% of a fossil's total surface area (often compromising sample integrity) whereas the non-destructive synchrotron-based techniques image 100% of a sample and the surrounding matrix.[16] Structural approaches cannot spatially resolve information on the intensity and distribution of either the chemical inventory or the pigment density (patternation) and rely upon qualitative predictions based upon structural data from extant bird feathers.[13] The subtle variation in pigment concentration and distribution can only be spatially resolved using SRS-XRF mapping, coupled with an understanding of organic sulphur inventory through XANES. This study shows that a non-destructive chemical approach is crucial to fossil pigment studies and should augment structural analysis when diagnosing pigment density and distribution. The synchrotron-based techniques used here have already shown, and will continue to provide invaluable data for studies attempting to characterise and distinguish the endogenous and exogeneous chemical components of tissues in many fields, including, palaeontology, archaeology, biology, and forensic investigations.

The Cu, Ni and organic S distributions in MB.Av.100 and HMN1880 are strongly controlled by feather structure, but only lighter elements (P and S) are comparable between all three specimens studied. These elemental patterns are most likely endogenous, and the fact that the Cu bonding environment in two of the specimens is consistent with organic chelation[16] implies that the trace metals in MB.Av.100 and HMN1880 are biomarkers for eumelanin pigmentation in *Archaeopteryx*. There is a distinct plumage pattern of dark pigment in the outer vain and tips, while the inner vane (protected by overlapping feathers) remains relatively un-pigmented (Fig. 1E and Fig. 3). This supports a possible visual role for pigments in the feathers of *Archaeopteryx*, potentially acting as a fitness criterion in the natural selection of this species, impacting upon the evolution of pigmentation in this and other feathered theropod dinosaurs.

Acknowledgements

Funding was provided by NERC supporting HEB, NERC Enviro-synch-2 and an anonymous donor. We gratefully acknowledge Peter Barrett for the development of the Velocirastor visualization software.

References

1 C. M. A. Darwin, *On the Origin of Species by Means of Natural Selection, or the Preservation of Favoured Races in the Struggle for Life*, London, 1859.
2 P. Berthold, G. Mohr and U. Querner, *Naturwissenschaften*, 1996, **83**, 568–570.
3 C. L. Ralph, *Am. Zool.*, 1969, **9**, 521.
4 K. J. McGraw, *Bird Colouration*, Boston, 2003, pp. 243–294.
5 J. D. Simon, D. Peles, K. Wakamatsu and S. Ito, *Melanoma Res.*, 2009, **22**, 563.
6 P. A. Riley, *Int. J. Biochem. Cell Biol.*, 1997, **29**, 1235–1239.
7 A. Sanchez-Ferrer, J. N. Rodriguez-Lopez, F. Garcia-Canovas and F. Garcia-Carmona, *Biochim. Biophys. Acta*, 1995, **1247**, 1–11.
8 K. J. McGraw, R. J. Safran and K. Wakamatsu, *Funct. Ecol.*, 2005, **19**, 816–821.
9 J. P. Trinkaus, *J. Exp. Zool.*, 1948, **109**, 135–170.
10 S. Ito, *Pigm. Cell Res.*, 2003, **16**, 230–236.
11 F. Zhang, S. L. Kearns, P. J. Orr, M. J. Benton, Z. Zhou, D. Johnson, X. Xu and X. Wang, *Nature*, 2010, **463**, 1075–1078.
12 Q. Li, K. Q. Gao, J. Vinther, M. D. Shawkey, J. A. Clarke, L. D'Alba, Q. Meng, D. E. G. Briggs and R. O. Prum, *Science*, 2010, **327**, 1369–1372.
13 R. M. Carney, J. Vinther, M. D. Shawkey, L. D'Alba and J. Ackermann, *Nat. Commun.*, 2012, **3**, 637.
14 B. H. Willier and M. E. Rawles, *Physiol. Zool.*, 1940, **13**, 177–202.
15 J. A. Clarke, D. T. Ksepka, R. Salas-Gismondi, A. J. Altamirano, M. D. Shawkey, L. D'Alba, J. Vinther, T. J. DeVries and P. Baby, *Science*, 2010, **330**, 954–957.
16 R. A. Wogelius, P. L. Manning, H. E. Barden, N. P. Edwards, S. M. Webb, W. I. Sellers, K. G. Taylor, P. L. Larson, P. Dodson, H. You, L. Da-qing and U. Bergmann, *Science*, 2011, **333**, 1622–1626.
17 P. Wellnhofer, *Archaeopteryx: The icon of evolution*, Berlin, 2009.
18 H. Meyer, *Neues Jb Miner., Geon., Geol., Pet.-Kunde*, 1861, 678–679.
19 H. Meyer, *Neues Jb Miner., Geon., Geol., Pet.-Kunde*, 1861, 561.
20 H. Meyer, *Palaeontographica*, 1862, **10**, 53–56.
21 U. Bergmann, R. W. Morton, P. L. Manning, W. I. Sellers, S. Farrar, K. G. Huntley, R. A. Wogelius and P. Larson, *Proc. Natl. Acad. Sci. U. S. A.*, 2010, **107**, 9060–9065.
22 H. Tischlinger and D. Unwin, *Archaeopteryx*, 2004, **22**, 17–50.
23 N. P. Edwards, H. E. Barden, B. E. van Dongen, P. L. Manning, P. L. Larson, U. Bergmann, W. Sellers and R. A. Wogelius, *Proc. R. Soc. London, Ser. B*, 2011, **278**, 3209–3218.
24 N. P. Edwards, R. A. Wogelius, U. Bergmann, P. L. Larson, W. I. Sellers and P. L. Manning, *Appl. Phys. A*, 2013, **111**(1), 147–155.
25 M. Sandström, F. Jalilehvand, E. Damian, Y. Fors, U. Gelius, M. Jones and M. Salomé, *Proc. Natl. Acad. Sci. U. S. A.*, 2005, **102**, 14165–14170.
26 G. K. R. Goldstein, B. A. B. Flory, M. Samia, J. M. Ichida and E. H. Burtt, *Auk*, 2004, **121**, 656–659.
27 P. Davis and D. E. G. Briggs, *Palaios*, 1998, **13**, 3–13.
28 P. L. Manning, P. M. Morris, A. McMahon, E. Jones, A. Gize, J. H. S. Macquaker, J. Marshall, T. Lyson, G. Wolff, M. Buckley and R. A. Wogelius, *Proc. R. Soc. London, Ser. B*, 2009, **276**, 3429–3437.
29 J. Sagemann, B. B. Jørgensen and O. Greeff, *Geomicrobiology*, 1998, **15**, 85–100.
30 A. J. Kear, D. E. G. Briggs and D. T. Donovan, *Palaeontology*, 1995, **38**, 105–131.
31 T. Lingham-Soliar, R. H. C. Bonser and J. Wesley-Smith, *Proc. R. Soc. London, Ser. B*, 2010, **227**, 1161–1168.
32 T. Lingham-Soliar and J. Glab, *Palaeogeogr., Palaeoclimatol., Palaeoecol.*, 2010, **291**, 481–487.
33 L. Hong and J. D. Simon, *J. Phys. Chem. B*, 2007, **111**, 7938–7947.
34 J. Horcicko, J. Borovanský, J. Duchon and B. Procházková, *Hoppe-Seyler's Z. Physiol. Chem.*, 1973, **354**, 203–204.
35 C. A. Flemming and J. T. Trevors, *Water, Air, Soil Pollut.*, 1989, **44**, 143–158.
36 E. H. Burtt and J. M. Ichida, *Condor*, 2004, **106**, 681–686.
37 ICZN, *Bull. Zool. Nom.*, 2011, **68**(3), 230–233.